A&A, 712, C2 (2026)
https://doi.org/10.1051/0004-6361/202661646e

Astronomy & Astrophysics

Flaires

A comprehensive catalog of dust echo-like infrared flares *(Corrigendum)*

J. Necker[1,2,⋆], E. Graikou[1], M. Kowalski[1,2], A. Franckowiak[3], J. Nordin[2], T. Pernice[1,2], S. van Velzen[4], and P. M. Veres[3]

[1] Deutsches Elektronen Synchrotron DESY, Platanenallee 6, 15738 Zeuthen, Germany
[2] Institut für Physik, Humboldt-Universität zu Berlin, 12489 Berlin, Germany
[3] Fakultät für Physik & Astronomie, Ruhr-Universität Bochum, 44780 Bochum, Germany
[4] Leiden Observatory, Leiden University, Postbus 9513, 2300 RA, Leiden, The Netherlands

A&A, 695, A228 (2025), https://doi.org/10.1051/0004-6361/202451340

Key words. accretion, accretion disks – catalogs – galaxies: active – infrared: galaxies – errata, addenda

Table 1. Number changes beyond 10^{-3} of the expected factor per affected column.

	New	Missing	Changed
PeakLbol	5	5	22
Ebol	7	10	43
Fluencebol	7	10	45
PeakTime	5	5	14

Notes. New measurements were obtained where the MCMC fits now converge. Conversely, for the missing objects, the MCMC fits that had previously converged now do not.

Equation (7) was missing a factor of 2 in the analysis code. This led to an overestimation of the blackbody radius, $R_{\rm eff}$, by a factor of $\sqrt{2}$, and an overestimation of the bolometric blackbody luminosities, $L_{\rm bol}$, by a factor of 2. The measured temperatures are not affected, so the qualitative evolution of the light curves remains unchanged (see Figs. 3 and 4). However, because the Markov chain Monte Carlo (MCMC) fits rely on random moves in the parameter space, for 85 objects (around 10% of the sample) fits for up to two epochs converged where they had not before, and vice versa. As this occurred for the epochs where the flare is barely detectable, the peak bolometric luminosity was mostly unaffected. However, because the bolometric energy is a sum over the measured luminosities (Eq. (8)), for these objects it changed beyond the expected factor of 0.5. For 14 objects, the peak time of the bolometric luminosity also changed as a result. The exact changes per column are listed in Table 1.

The conclusions about the nature of the transients are not affected: the evolution of the blackbody radius, temperature, and luminosity remain consistent with cooling dust after illumination by Tidal Disruption Event (TDE) emission (Fig. 5). The energy remains in the range of 10^{51}–10^{52} erg (Fig. 6), consistent with the energy output of a TDE, assuming a covering factor of $f_c \gtrsim 0.1$, the disruption of a solar mass star, subsequent accretion of half its mass, and a dissipation efficiency of $\epsilon \approx 0.1$. The comparison between the blackbody radius at peak, $R_{\rm eff,peak}$, and the radius derived from the light curve, $R_{\rm LC}$, now fall even better in the parameter space for the width of the activating flare $O(10\,{\rm d}) < \Delta T_{\rm opt} < O(100\,{\rm d})$ (Fig. 7) expected for TDEs. The correlations between the dust radius, temperature, measured energy, and luminosity did not change significantly (Fig. 8).

After changing the luminosity completeness threshold from 6×10^{43} erg s^{-1} to 3×10^{43} erg s^{-1}, as expected for a missing factor of 2, the implications for the transient rate and its evolution with redshift remain unaffected. For completeness, the updated Figs. 10, 11, and 12 are also shown below.

Data availability

The updated Table A.1 is available at the CDS via https://cdsarc.cds.unistra.fr/viz-bin/cat/J/A+A/712/C2.

Acknowledgements. We thank Hui Liu for detailed comparisons of the dust echo in SDSS J010320.39+140152.5 that helped us discover the erroneous code.

⋆ Corresponding author: necker@strw.leidenuniv.nl

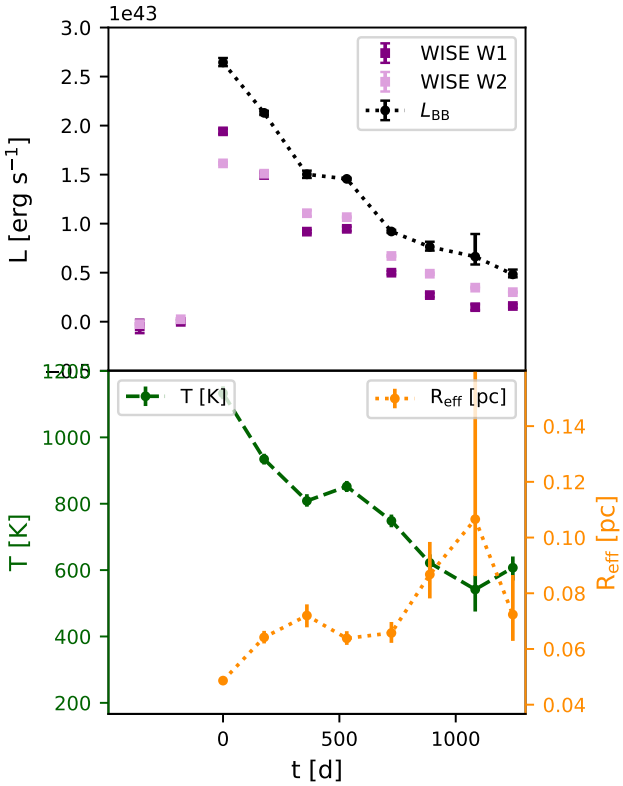

Fig. 4. Light curve and evolution of $R_{\rm eff}$ and T for NGC 7392. The crosses mark the best-fit values of the visits where the MCMC sampling did not result in a meaningful constraint of $L_{\rm bol}$.

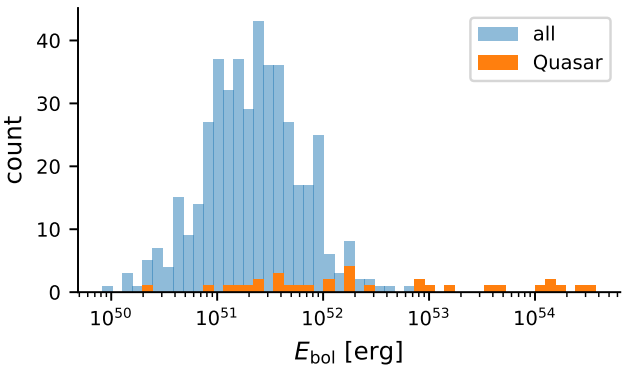

Fig. 6. Distribution of the total emitted energy, assuming hot dust. The quasars are identified by a match to Milliquas.

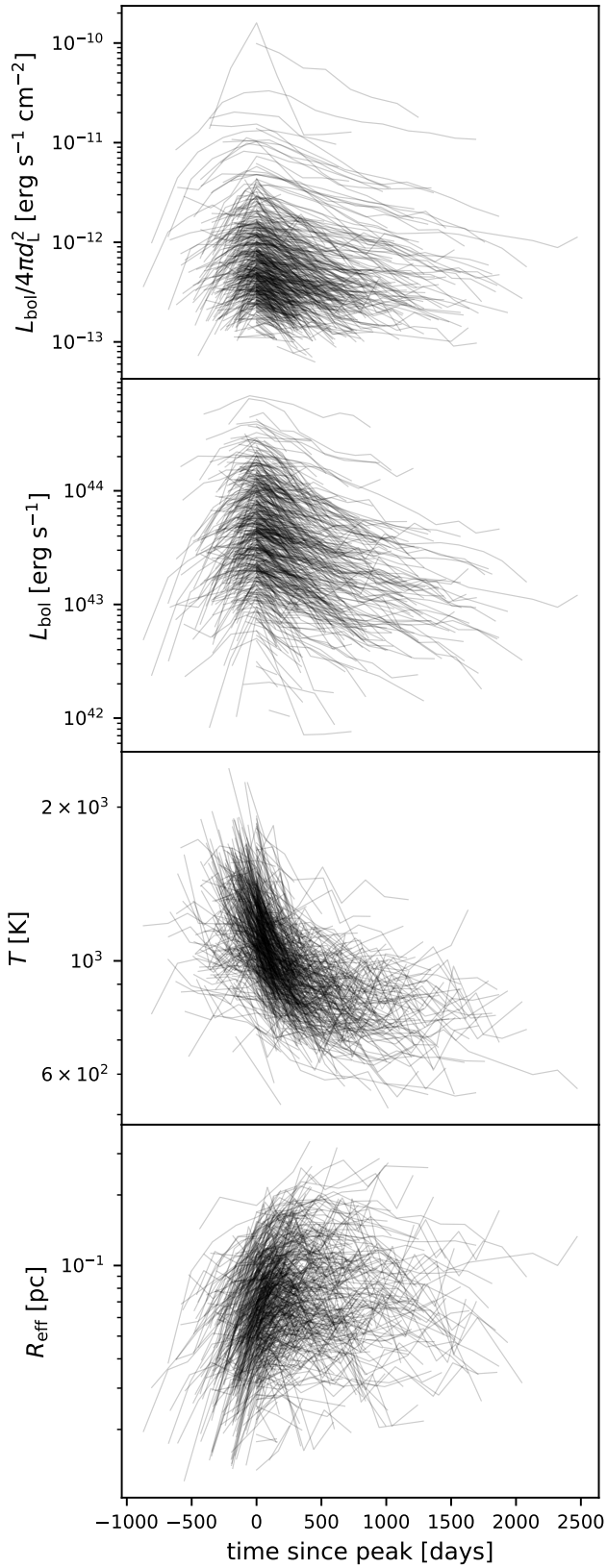

Fig. 5. Parameters from the blackbody fits for 449 sources where at least two epochs have a good fit. The time is given in the source frame. First panel: bolometric flux based on the bolometric luminosity and the luminosity distance. Second panel: bolometric luminosity. Third and fourth panel: temperature and effective radius.

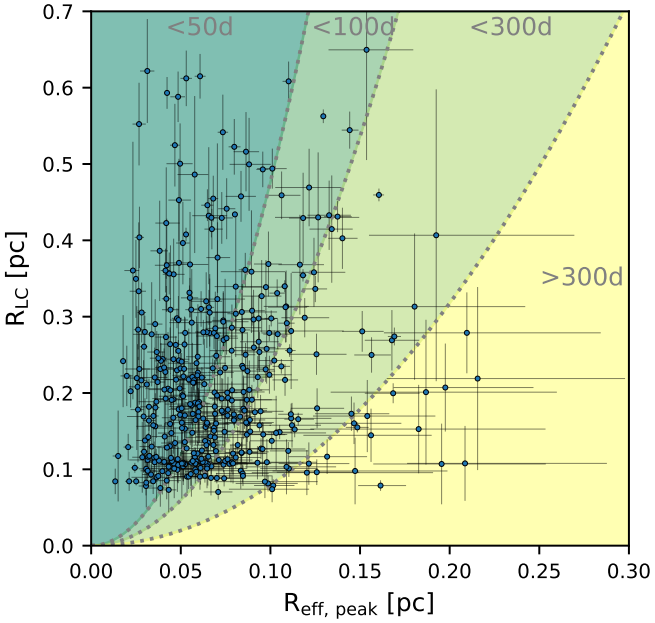

Fig. 7. Dust radius estimated from the IR light curve, R_{LC}, against the radius at the peak, $R_{eff,\,peak}$, obtained from the blackbody fits. The colored contours represent the actual blackbody radius for a finite width of the initial O/UV transient.

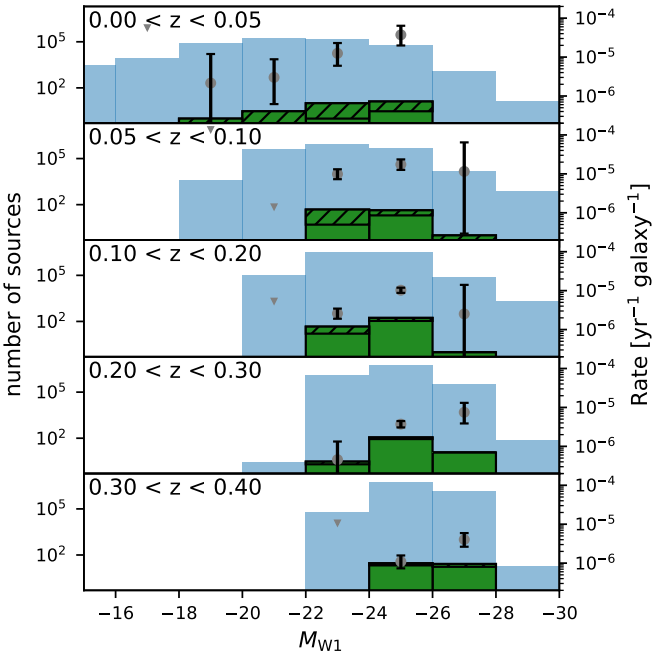

Fig. 10. Rate as a function of the absolute magnitude in W1 and redshift. The light blue histogram shows the total number of galaxies in the parent galaxy sample, and the green histogram shows the host of our flare sample. The black-hatched bars represent flares with $L_{bol,\,peak} < 3 \times 10^{43}$ erg. The gray data points and black error bars show the rate as calculated with Eq. (12). The gray triangles represent the 90% upper limit on the rate where no flare was observed. The errors are statistical only.

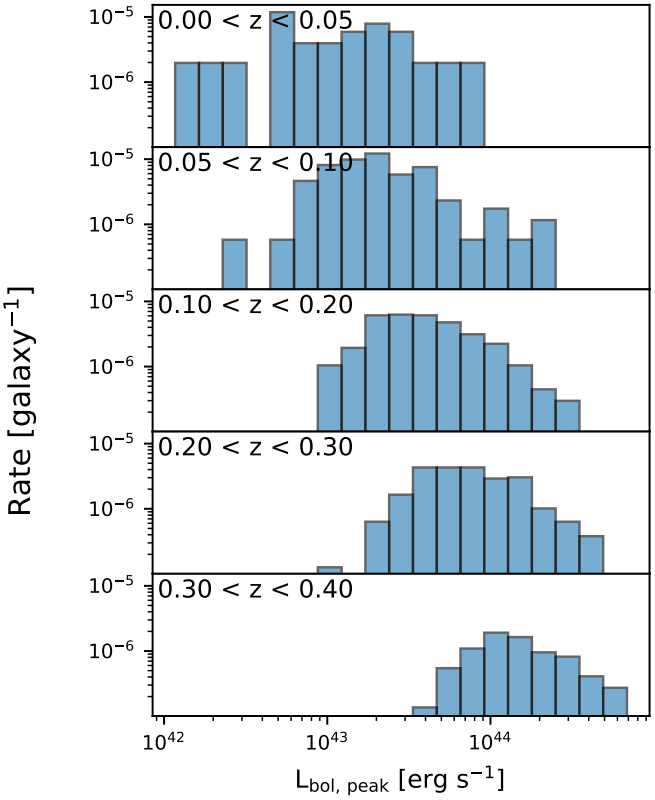

Fig. 11. Distribution of the maximum bolometric luminosity as a function of redshift.

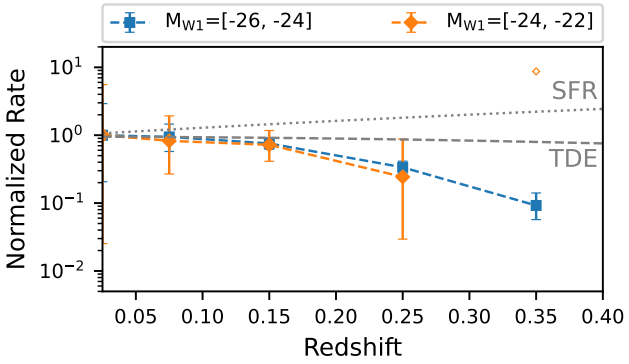

Fig. 12. Evolution of the rate with redshift for the two M_{W1} bins with flares in the first and at least one other redshift bin, normalized to the first redshift bin. The open symbols represent upper limits. The redshift evolution of the star formation rate (SFR) and for the TDEs is shown for comparison.

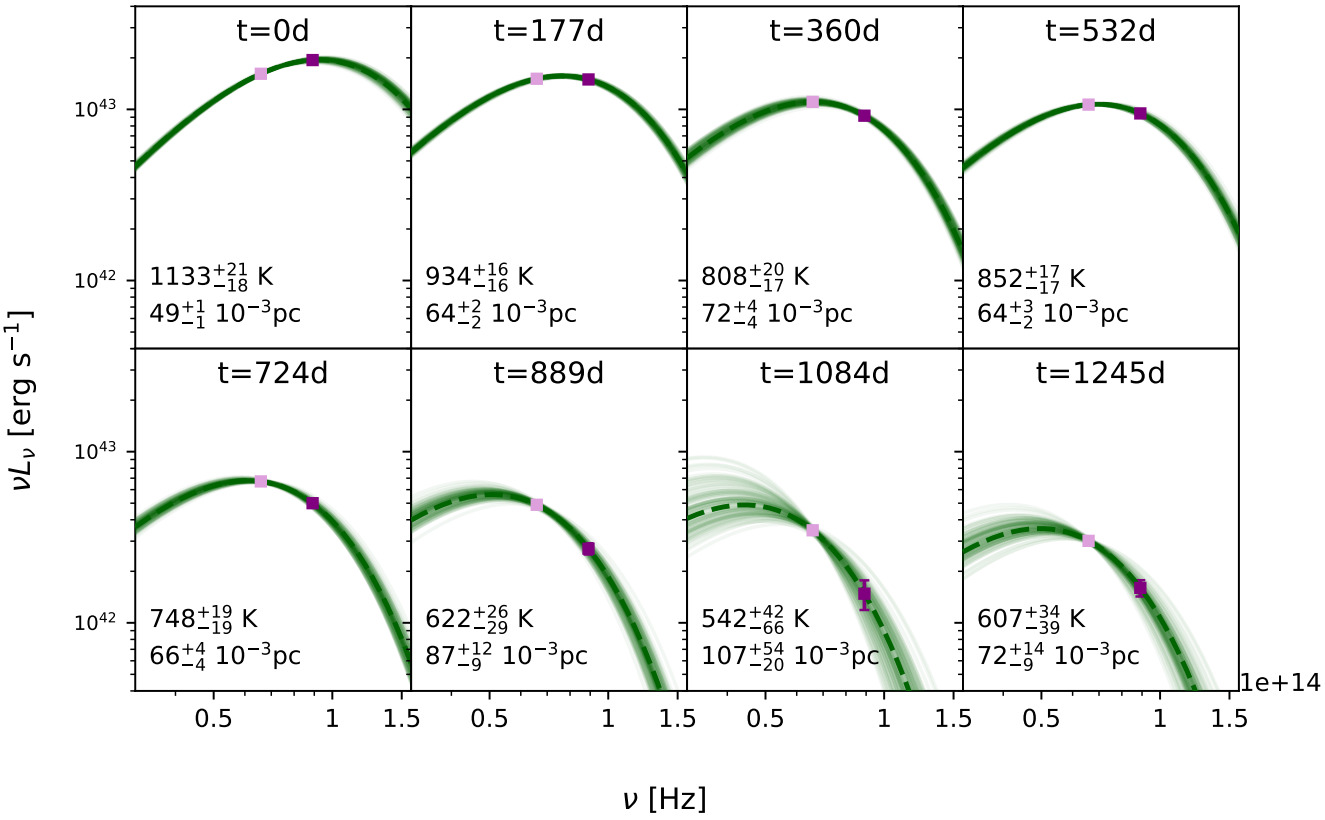

Fig. 3. Blackbody fits for NGC 7392 for all epochs of the flare where the MCMC sampling resulted in meaningful constraints on the fit parameters. The dashed green line shows the best fit, and the transparent lines show the results from the MCMC sampling. The best fit and 68th percentile temperature and effective radius values are shown in the bottom left corner. The frequency, ν, is given in the source frame.

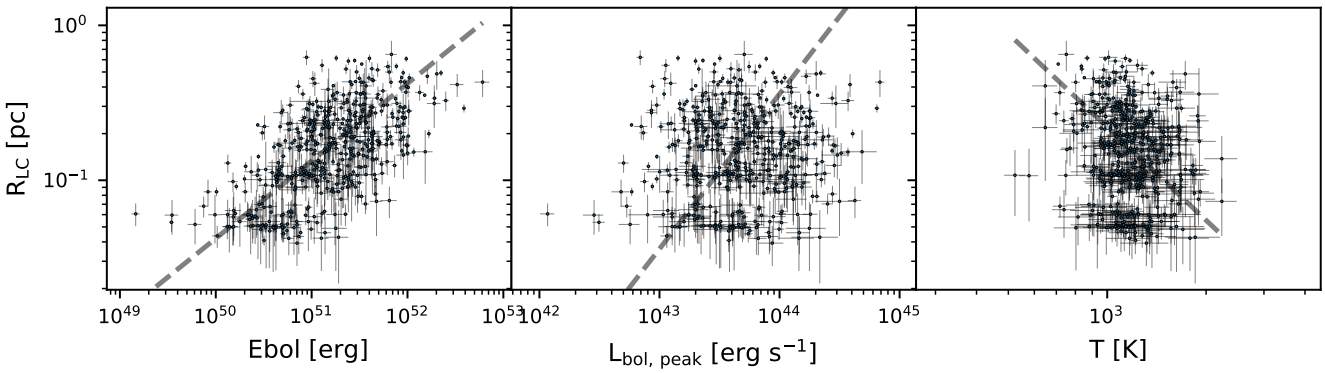

Fig. 8. Correlation of the total emitted bolometric energy E_{bol}, the peak bolometric luminosity, $L_{bol,\,peak}$, and the dust radius inferred from the light curve R_{LC}. The dashed lines represent the theoretically expected relations.